Available online at www.sciencedirect.com
SCIENCE DIRECT
Journal of Catalysis 234 (2005) 376–384
JOURNAL OF CATALYSIS
www.elsevier.com/locate/jcat

Influence of support ionicity on the hydrogen chemisorption of Pt particles dispersed in Y zeolite: consequences for Pt particle size determination using the H/M method

Yaying Ji [a,1], Ad M.J. van der Eerden [a], Vincent Koot [a], Patricia J. Kooyman [b], Johannes D. Meeldijk [a], Bert M. Weckhuysen [a], Diek C. Koningsberger [a,*]

[a] *Department of Inorganic Chemistry and Catalysis, Debye Institute, Utrecht University, PO Box 80083, 3508 TB Utrecht, The Netherlands*
[b] *National Centre for High Resolution Electron Microscopy, Rotterdamseweg 137, 2628 AL Delft, The Netherlands*

Received 28 April 2005; revised 24 June 2005; accepted 27 June 2005

Available online 10 August 2005

Abstract

Zeolite Y-supported Pt particles were studied by high-resolution transmission electron microscopy (HRTEM), extended X-ray absorption fine structure (EXAFS), and H_2 chemisorption experiments. The ionicity (i.e., electron richness of the zeolite oxygen atoms) was altered by using different cations (NaY, MgY, and LaY) and by steaming and introduction of protons (H-USY). Highly dispersed Pt particles were introduced inside the zeolite pores using a very careful synthesis procedure. Computer analysis of HRTEM images exhibited similar Pt particle size distributions with calculated average Pt particle sizes ranging from 0.98 to 1.26 nm for the various zeolite Y-supported Pt particles. The EXAFS results revealed that the first-shell Pt–Pt coordination number was around 6.5, in good agreement with the observed HRTEM results. H_2 chemisorption experiments found a much higher H/Pt value for Pt/NaY (1.63) than for Pt/H-USY(0.88), implying no relationship with the Pt dispersion as determined by HRTEM. Using the values for the dispersion (Pt_s/Pt) as calculated from the HRTEM results, one can obtain a value for the number of chemisorbed hydrogen atoms per surface platinum atom (H/Pt_s ratio). This value demonstrates a clearly decreasing trend with decreasing electron richness of the support oxygen atom: 1.96 (Pt/NaY) > 1.74 (Pt/MgY) > 1.51 (Pt/LaY) > 1.11 (Pt/H-USY). These results indicate that the hydrogen coverage on supported Pt particles depends strongly on the support ionicity. This has significant consequences for the catalytic behavior of hydrogenolysis and hydrogenation reactions catalyzed by Pt. These results also indicate that one should be cautious in interpreting H_2 chemisorption results only in terms of Pt dispersion. This approach is valid only when comparing Pt particles dispersed on the same support. Serious deviations in the real Pt dispersions occur if Pt is supported on oxides with different ionicities.

Keywords: Hydrogen chemisorption; H/M method; High-resolution transmission electron microscopy; Particle size determination; Metal–support interaction; Support ionicity

1. Introduction

It has been well established in the literature [1–9] that the nature of the support influences the rate of hydrogenation and hydrogenolysis reactions on catalytically active metal particles. In the conversion of neopentane ($C–(CH_3)_4$), it has been observed that the rate of hydrogenolysis is several orders of magnitude higher when Pt particles are supported on an acidic support compared with on a basic support. In addition, inhibition of the hydrogenolysis of alkanes by hydrogen is much stronger for basic supports; the order in H_2 ranges from −2.5 (basic support) to −1.5 (acidic) [9–12]. Explanations for this finding have involved the formation of metal–proton adducts on Brønsted acidic supports [4,13], electron transfer between support and particle [3,14,15], po-

* Corresponding author. Fax: +31-30-2511027.
E-mail address: d.c.koningsberger@chem.uu.nl (D.C. Koningsberger).
[1] Present address: Department of Chemical Engineering, University of Virginia, Charlottesville, VA 22904-4741, USA

0021-9517/$ – see front matter
doi:10.1016/j.jcat.2005.06.030

larization of the metal particles by nearby cations [16], and a change in the ionization potential of the metal due to a shift in the d-band density of states [7,8,17,18].

Work by our group revealed that the nature of the metal–support interaction involves a change in the electronic properties of the metal cluster, induced by and correlated with the electron richness of the support oxygen atoms [7,8,17,19]. This oxygen electron richness is determined primarily by the ionic character of the cations in the oxide support; with electron-rich oxygens existing in basic supports with alkaline cations and electron-poor oxygens existing in acidic supports with protons or other, more covalent cations. A new analysis procedure of the Pt L_2 and L_3 near-edge structure (XANES), atomic X-ray absorption fine structure (AXAFS), and density functional theory (DFT) calculations on supported Pt clusters revealed that increasing electron richness of the support oxygen atoms affects the electronic properties of a metal particle in at least three separate ways: (i) the complete Pt density of states shifts to higher energy (lower binding energy) [7,8]; (ii) the location of the $6s, p$ bonding orbital (i.e., the interstitial bonding orbital [20]) moves from the metal–support interface to the surface of the Pt particles [17]; and (iii) the insulator-to-metal transition is occurring at lower particle sizes [21]. This knowledge, together with information on the dominant hydrogen adsorption sites (atop or n-fold) obtained from the Pt L_3 XANES calculations, was used to analyze previously reported neopentane hydrogenolysis kinetic data [9]. The results from this analysis provided a basic understanding of the metal–support interaction for hydrogenolysis reactions of alkanes catalyzed by Pt particles on supports with different ionicities and acid/base properties.

DFT calculations show that the Pt–H bond strength is greater on ionic supports (basic, with electron-rich O atoms), implying higher H coverage compared with covalent supports (acidic, with electron-poor O atoms) [22]. The combination of DFT calculations with the new XANES analysis procedure applied to EXAFS data on small supported Pt particles ($n < 6.5$) led to detailed insights into the correlation between the ionicity of the support and the type of active sites for H chemisorption [23]. At very low H_2 pressure or high temperature, the strongest-bonded H is chemisorbed in an atop position. With decreasing temperature or at higher H_2 pressure, only n-fold ($n = 2$ or 3) sites are occupied. At high H_2 pressure or low temperature, the weakest-bonded H is positioned in an "on-top" site, with the chemisorbing Pt already having a stronger bond to an H atom in an n-fold site. The results of the new XANES analysis and the DFT calculations both suggest that the hydrogen coverage, which exists on the Pt surface at high-temperature catalytic reaction conditions, depends strongly on the ionicity of the support. Because Pt particles on acidic supports are the most active in hydrogenation and hydrogenolysis reactions, it is entirely possible that the difference in catalytic activity is related to differences in H chemisorption properties [9].

In this study the chemisorption of hydrogen on small Pt particles dispersed in Y zeolite is quantitatively determined using the conventional H/M technique. Highly dispersed Pt particles were introduced inside the zeolite pores by applying a very careful synthesis procedure to obtain a narrow particle size distribution. The electron richness of the zeolite oxygen atoms was systematically decreased by changing the charge-compensating ion from Na^{1+}, Mg^{2+}, La^{3+}. Finally, the lowest electron richness of the zeolite oxygen atoms was obtained with a Pt/H-USY with extra-framework Al and Brönsted acid sites. The particle size distribution and average particle size were determined by high-resolution transmission electron microscopy (HRTEM). EXAFS was used as an additional tool to determine the average Pt–Pt coordination number. The results show that the difference in dispersion of the four samples was not more than 12.5%, but the experimental H/M values decreased systematically from 1.63 for Pt/NaY to 0.87 for Pt/H-USY. This implies that (i) the hydrogen coverage for the same-sized Pt particles is a strong function of the electron richness of the support oxygen atoms, and (ii) the H/M technique does not give reliable information about the dispersion of Pt particles when comparing Pt particles on supports with different ionicities.

2. Experimental

2.1. Catalyst preparation

NaY (LZY 54) and NH_4-USY (LZY 84) supports were obtained commercially; their properties are given in Table 1. MgY was prepared by four successive ion exchanges for 12 h with an aqueous 1 mol solution of $MgCl_2$ (UCB. P.a.). The sample was washed chlorine-free and dried in air at room temperature overnight. Chemical analysis indicated that after four successive ion exchanges, the degree of exchange was >98% (more details for MgY have been provided elsewhere [24]). The LaY sample was prepared by two successive ion exchanges with a solution of $La(NO_3)_3$. pH was controlled to >4 to avoid acid dealumination or sieve destruction. The exchanged zeolites were washed to remove

Table 1
Properties of zeolite Y supported Pt catalyst

Catalyst	Na (wt%)	(Si/Al) total	Al_F (mmol/g)	Al_{EF} (mmol/g)	Acid sites (mmol/g)	S_{BET} (m^2/g)	Pores (ml/g)	
							micro	meso
Pt/NaY	10	2.5	4.3	0	0	908	0.34	0.03
Pt/H-USY	0.1	2.5	2.6	2.2	1.4	755	0.26	0.1

F, framework; EF, extra framework.

excess salts before being heated to 100 °C for drying. The final La loading amounted 20 wt% (more details for LaY have been provided elsewhere [25]). The crystallinity for both samples was checked with X-ray diffraction and scanning electron microscopy techniques.

The zeolite powder was dried in a flask at ∼200 °C in dynamic vacuum for two hours. Before the evacuation treatment is stopped, any water condensed at the outlet of the flask must be removed, to avoid water readsorption on the dried support. After the support cooled to room temperature, an aqueous solution of $Pt(NH_3)_4(NO_3)_2$ (Aldrich), containing an amount of Pt to provide a 1 wt% loading in the zeolite, was injected on the dry support in static vacuum. The volume of the injected solution was 95% of the total pore volume, to maximize the fluid uptake into the pores. The impregnated samples were thoroughly shaken, air was admitted, and the samples were kept at room temperature overnight.

Next the zeolite samples were dried at 80 °C for 8 h in flowing N_2 in a rotating vaporizer. A sieve fraction (212–425 μm) was dried at 150 °C for 8 h. The sample was then heated with a ramp of 0.2 °C/min from 150 to 300 °C and calcined at 300 °C for 1 h. A high space velocity of the O_2/N_2 (20%) mixture gas was needed during drying and calcinations, to maximize the desorption rate of water and NH_3. The need for an extremely low heating rate and high space velocity has been discussed in depth elsewhere [26]. For Pt/H-USY, a final temperature of 350 °C was used for calcinations, to remove ammonia from the acid sites of NH_4-USY to obtain H-USY. After calcination, the sample was cooled to room temperature in the flowing mixture of O_2/N_2. Subsequently, the calcined samples were reduced in pure H_2 gas by heating with a ramp of 5 °C/min to 300 °C and maintaining this temperature for 2 h. After reduction, the sample was first cooled to room temperature in flowing hydrogen, then flushed with a high flow of N_2, and finally passivated by adding a small flow of O_2 into the flowing N_2.

2.2. HRTEM

HRTEM was performed using a Philips CM 30 UT electron microscope with a field emission gun as the source of electron operated at 300 kV. Samples were mounted on a microgrid carbon polymer supported on a copper grid by placing a few droplets of a suspension of ground sample in ethanol on the grid, followed by drying at ambient conditions.

Particle size analysis was done using the Soft Imaging Systems AnalySIS software. Positive photographic images were scanned at 150 dpi. A selection was made, and a $N \times N$ filter was applied. This image was subtracted from the original selection to level the background. After this, a Fourier filter enhanced the contrast of the particles. Gray-value detection then identified the particles for which the size was automatically determined by the software and statistically processed. The limit of accuracy in the size of the Pt particles as determined with the software analysis is an estimated 0.1 nm.

2.3. EXAFS data collection and data-analysis

EXAFS data were collected at the Pt L_3- and L_2-edge using beamline X1.1 of the HASYLAB synchrotron (Hamburg, Germany) equipped with an Si(311) crystal. The monochromator was detuned to 50% of maximum intensity. All measurements were done in transmission mode using ion chambers filled with a N_2/Ar mixture to have an X-ray absorbency of 20% in the first and of 80% in the second ion chamber. At the Pt L_3-edge (11,564 eV), the estimated resolution was 2 eV. To decrease low- and high-frequency noise as much as possible, an acquisition time of 0.5 s for the EXAFS data was used with a gradual increase to 1.5 s at high photon energy, and three scans were averaged.

The samples as prepared were pressed into self-supporting wafers (calculated to have a total absorbance of 2.5) and placed in a controlled atmosphere cell operated at 1 atm [27]. Subsequently, the catalysts were dried at 150 °C for 1 h, re-reduced in a hydrogen flow at 300 °C, and cooled to room temperature in a hydrogen flow. Then the hydrogen supply was disconnected from the cell, and the cell was cooled down to liquid nitrogen temperature to perform EXAFS measurement.

Extraction of the EXAFS data from the measured absorption spectra was done using the XDAP code [28]. Three scans were averaged, and the pre-edge was subtracted using a modified Victoreen curve. The background was subtracted using cubic spline routines with a continuously adjustable smooth parameter. Normalization was performed by dividing the data by the height of the absorption edge at 50 eV.

Data analysis was performed by multiple-shell fitting in R-space using the EXAFS data analysis program XDAP, which allows one to minimize the residuals between both the magnitude and the imaginary part of the Fourier transforms (FTs) of the data and the fit. R-Space fitting has significant advantages over the usually applied fitting in k-space [29]. The difference file technique was applied together with phase- and amplitude-corrected Fourier transforms to resolve the different contributions in the EXAFS data. In the difference file technique, one simultaneously fits all contributions, but each individual contribution is monitored and optimized with respect to the other contributions present in the EXAFS spectrum [29]. This allows also for a more accurate determination of the minor contribution to the EXAFS spectrum. Both high Z (Pt–Pt) and low Z (Pt–O) contributions are present in the EXAFS data collected on the Pt/Y samples [8]. The R-space fits were carried out by applying k^1 and k^3 weightings to ensure that the results were the same for all weightings. A k^3 weighting emphasizes the high Z contributions to the spectrum, whereas a k^1 weighting focuses on the low Z contribution.

Theoretical phase shifts and backscattering amplitudes for the Pt–Pt and Pt–O absorber–scattering pairs were used

Table 2
FEFF7 parameters used to calculate Pt–Pt and Pt–O theoretical references. The references were calibrated using Pt-foil and $Na_2Pt(OH)_6$ [29]

Atom pair	Potential	σ^2 (Å^2)	S_0^2	V_r (eV)	V_i (eV)
Pt–Pt	Dirac–Hara	0.00234	0.82	−4.2	3.0
Pt–O	Dirac–Hara	0.00342	0.90	0.0	3.0

in EXAFS data analysis, which were generated utilizing the FEFF7 code with the parameters listed in Table 2 [29]. The theoretical references were calibrated with the aid of the experimental data of Pt foil and $Na_2Pt(OH)_6$ using a procedure reported previously [29].

2.4. Hydrogen chemisorption

Hydrogen chemisorption measurements were performed in a conventional static volume apparatus (Micromeritics ASAP 2010C). The samples were first dried under evacuation at 100 °C overnight, then reduced in pure H_2 at 300 °C for 1 h (ramp, 5 °C/min). The samples were evacuated at this temperature for 0.5 h, subsequently cooled down in vacuum to 36 °C at which temperature H_2 adsorption isotherms were taken. The absolute amount of adsorbed H_2 is determined from the decrease in pressure when adding a fixed volume of H_2 to a known volume containing a known amount of catalyst. The H/Pt ratios are obtained based on the adsorbed amounts of hydrogen determined with this isotherm by extrapolation of the linear part to zero pressure.

3. Results

3.1. HRTEM

The respective representative HRTEM images shown in Fig. 1 reveal that the Pt particles were uniformly dispersed in the support with a size around ∼1 nm. The software package "AnalySIS" was used to determine the particle size distribution from the HRTEM images as discussed earlier and to calculate the average Pt particle size. A large number of particles (350–450) could be examined, and good statistical values could be obtained. Fig. 2 shows that the Pt particles are distributed in the size range 0.6–2.0 nm and that the range 1–1.2 nm has the largest contribution. The calculated average particle diameters are 1.14 nm for Pt/NaY, 0.92 nm for Pt/MgY, 1.23 nm for Pt/LaY, and 1.26 nm for Pt/H-USY.

The Pt dispersion (i.e., the ratio of the number of surface Pt atoms [Pt(s)] to the total number of loaded Pt atoms [Pt(t)]) can be calculated from the average particle diameter. It is assumed that the supported Pt particles have a spherical shape with a face-centered cubic structure. The total number

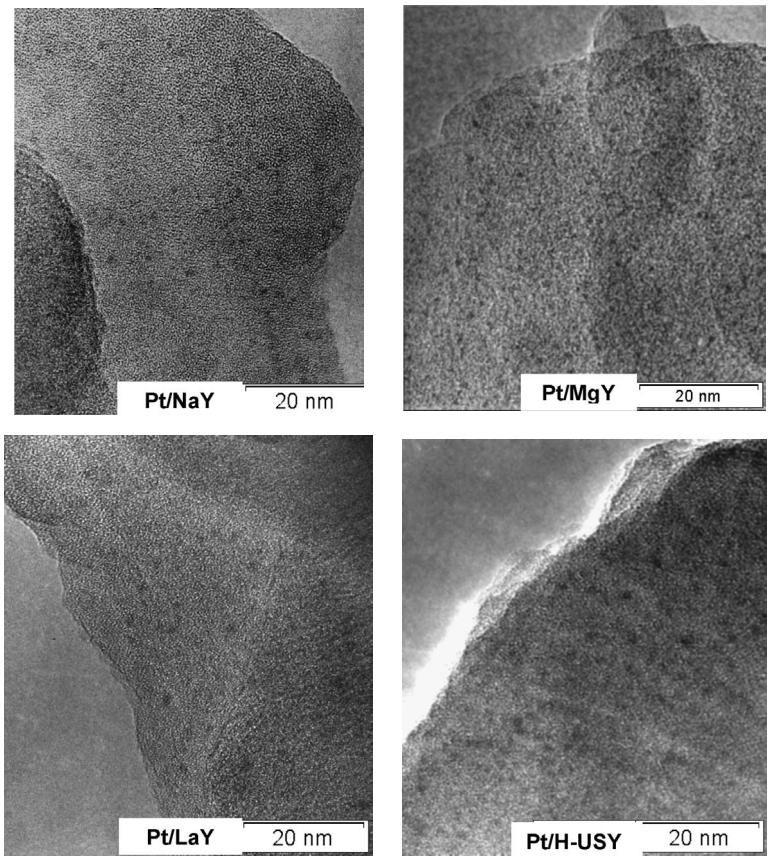

Fig. 1. HRTEM images of the Pt/Y samples. The length of the bar in each photograph is 20 nm.

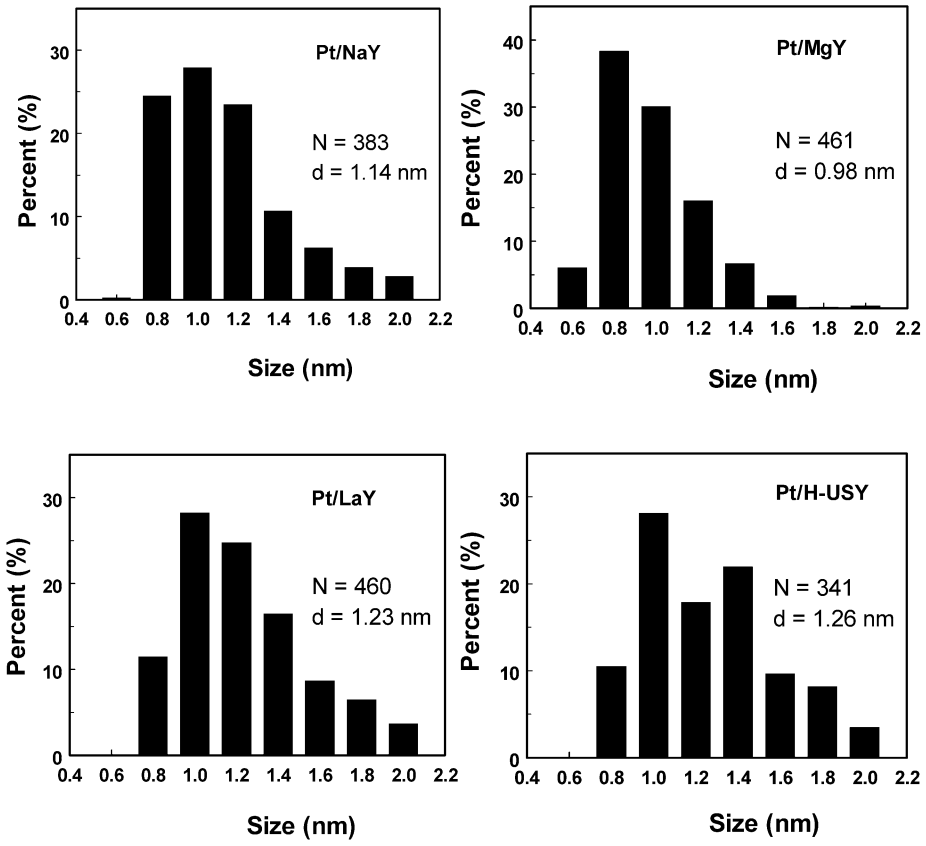

Fig. 2. Histograms with Pt particle size distribution of the Pt/Y samples obtained by computer analysis (350–450 Pt particles were analysed). d is average Pt particle size.

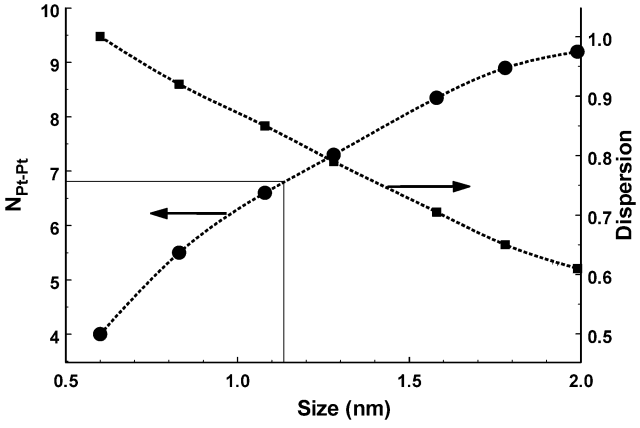

Fig. 3. Dispersion and first shell Pt–Pt coordination number ($N_{Pt–Pt}$) as a function of Pt particle size (diameter in nm) calculated with the help of the computer package Nubie [30]. Lines indicate data for Pt/NaY.

of atoms was calculated taking the diameter of the modeled particle as the particle size, and the number of surface atoms per particle was calculated using the definition of surface atoms having <12 neighboring atoms. A computer program [30] was used to obtain the relation between dispersion and average particle size (see Fig. 3). Using this relation, the dispersion was found to be 0.83 for Pt/NaY, 0.89 for Pt/MgY, 0.80 for Pt/LaY, and 0.79 for Pt/H-USY.

3.2. EXAFS

The raw EXAFS data are presented in Fig. 4a. The four samples have similar oscillation and similar node distances, pointing to a similar structure. The signal/noise ratio allows for EXAFS data analysis up to about $k = 13$ Å^{-1}, except for the Pt/LaY data, which can be analyzed only up to $k =$ 11 Å^{-1}. The corresponding FTs (k^1, $\Delta k = 3$–11 Å^{-1}) of the EXAFS spectra of the different zeolite-supported Pt particles are given in Fig. 4b. The shoulders at both the low and high R sides of the first Pt–Pt peak in the Fourier transform are due to the nonlinear Pt–Pt phase shift and the k dependence of the Pt backscattering amplitude [29]. It can be seen that the amplitudes of the magnitude of the FT occur in the order Pt/MgY < Pt/NaY < Pt/LaY < Pt/H-USY.

Multiple-shell fitting in R-space (FT: $\Delta k = 3$–13 Å^{-1}, $\Delta R = 1.6$–3.1 Å, except for Pt/LaY with $\Delta k = 3$–11 Å^{-1}), together with the difference-file technique, resulted in the identification of Pt and O backscatterers. There are eight free-fit parameters; this number is allowed because it is lower than the number of independent parameters according to the Nyquist theorem [29] ($N_{indp} = 11.5$, for Pt/LaY: 9.6). Minimizing the variances in imaginary and absolute parts led to the best fit. The variances of the fit of the imaginary part and absolute part are for all samples <1%. The quality of the fit for Pt/MgY shown in Fig. 5a is representative

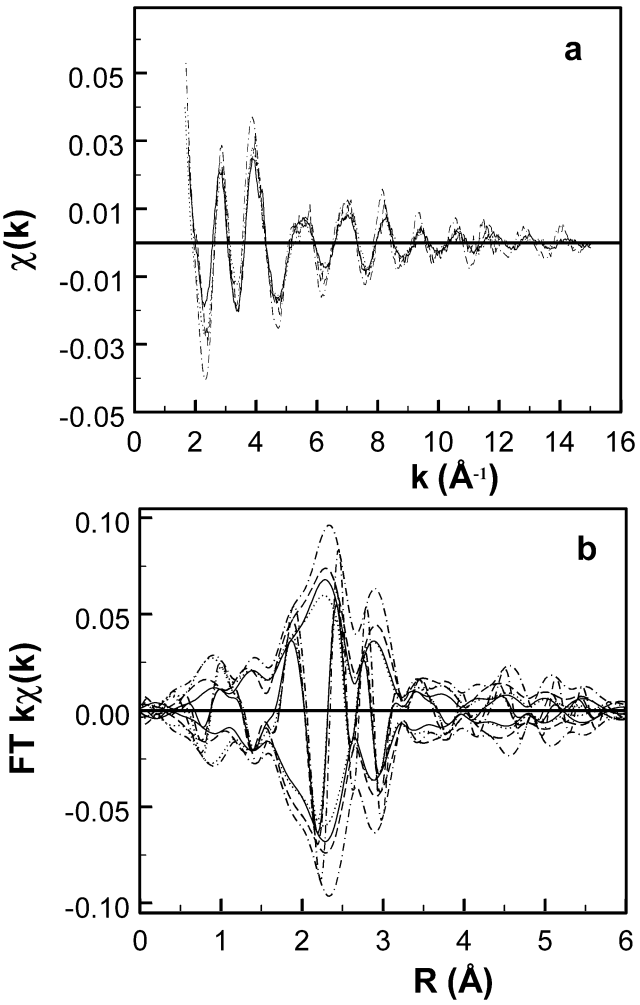

Fig. 4. (a) Experimental raw EXAFS data for Pt/NaY (solid line), Pt/MgY (dotted line), Pt/LaY (dashed line) and Pt/H-USY (dashed dotted line). (b) Corresponding Fourier transforms (k^1, $\Delta k = 3$–11 Å^{-1}). (samples are indicated with the same line type).

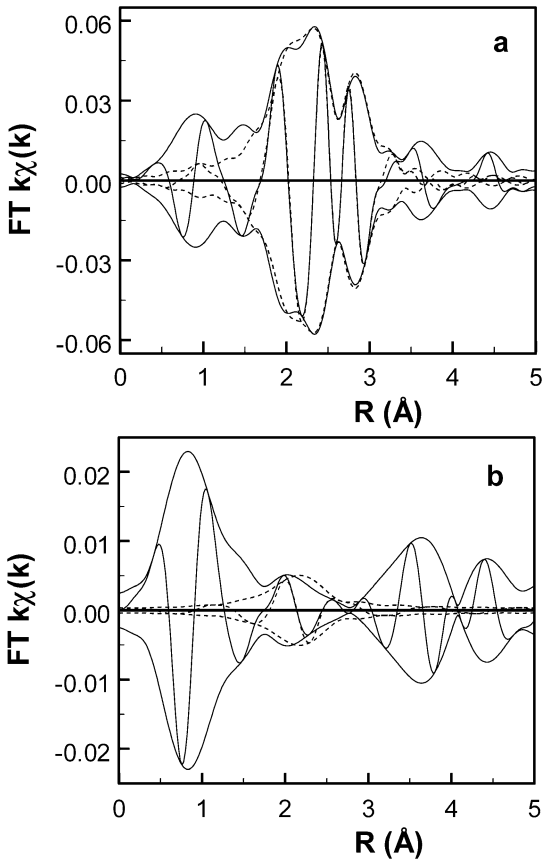

Fig. 5. (a) Fourier transform (k^1, $\Delta k = 3$–13 Å^{-1}) of the raw EXAFS data (solid line) and the total fit (Pt–Pt + Pt–O) (dotted line) for Pt/MgY. (b). Fourier transform (k^1, $\Delta k = 3$–9.5 Å^{-1}) of Pt–O difference file (raw EXAFS minus Pt–Pt) and fitted Pt–O contribution for Pt/MgY.

Table 3
EXAFS coordination parameters obtained from R-space fit (k^1, $\Delta k = 3$–13 Å^{-1}, $\Delta R = 1.6$–3.1 Å)

Catalyst	Scatter	N (±10%)	R (Å) (±0.02)	$\Delta\sigma^2$ (Å^2) ($\times 10^3$, ±5%)	E_0 (eV) (±10%)	Variance	
						Im.	Abs.
Pt/NaY	Pt	6.1	2.73	5.6	2.2	0.62	0.32
	O	0.6	2.71	3.0	−2.0		
Pt/MgY	Pt	6.3	2.65	6.1	2.7	0.46	0.28
	O	0.4	2.59	3.0	10.7		
Pt/LaY	Pt	7.1	2.75	5.6	1.7	0.47	0.14
	O	0.5	2.53	3.0	10.0		
Pt/HUSY	Pt	7.4	2.75	2.7	2.7	0.15	0.12
	O	0.5	2.50	3.0	11.2		

for all samples. The FT of the difference file (raw data minus the fitted Pt–Pt EXAFS) (solid line) is given in Fig. 5b. This FT shows different peaks: AXAFS (∼0.7 Å) [7,8,17], Pt–O (∼2.2 Å), Pt–Pt_2 (the second Pt coordination shell, at ∼3.6 Å), and Pt–Pt_3 (the third Pt coordination shell, at ∼4.5 Å). The FT of the fitted Pt–O contribution (i.e., the fit in R-space for $1.6 < R < 3.1$ Å) is plotted with a dotted line. The resulting fit parameters are displayed in Table 3. The Pt–Pt coordination numbers can be related to the average Pt particle size. For all samples, a long Pt–O distance has been detected showing a systematic decrease with decreasing electron richness of the support oxygen (see Section 4).

3.3. H/M experiments

In the H/M experiments, first and second isotherms were measured. After the first isotherm was determined at 36 °C, the sample was evacuated at the same temperature for 1 h and then a second isotherm was measured. The difference between the first and second isotherms is related to strongly chemisorbed hydrogen, and the second isotherm is determined by weakly chemisorbed hydrogen. An example of the H/M data collected for the Pt/NaY sample is shown in Fig. 6. Generally, a hydrogen adsorption isotherm involves two types of hydrogen: chemisorbed and physisorbed. The amount of chemisorbed H can be obtained by extrapolating the linear part of isotherm to zero pressure. This procedure subtracts the physisorbed H from the total amount of adsorbed H. The value determined by the extrapolation is then used to calculate the H/Pt ratio. Table 4 gives the amount of

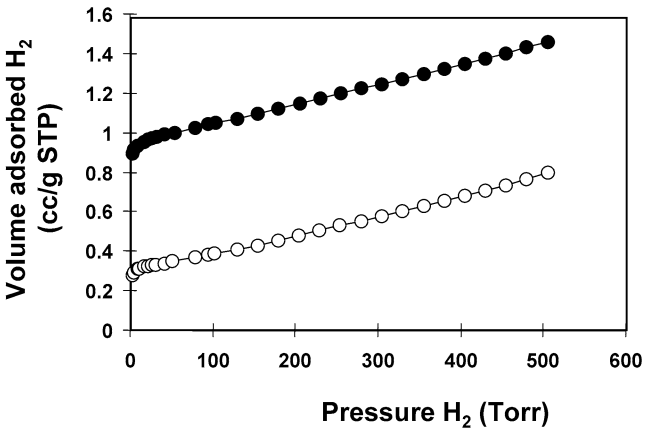

Fig. 6. First (solid circles) and second (open circles) hydrogen isotherm for Pt/NaY measured at 35 °C.

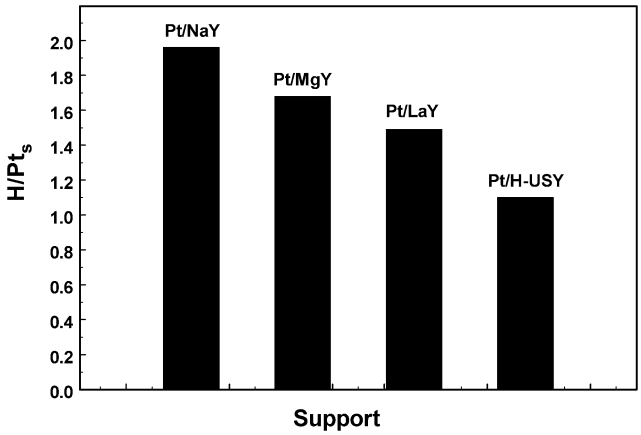

Fig. 7. Histogram of the number of chemisorbed H atoms per surface Pt atom calculated from experimental H/M values and Pt dispersions. The last values are obtained from the average Pt particle diameter determined by HRTEM (see Fig. 3).

chemisorbed H and the corresponding H/Pt ratios for these samples. The determined H/Pt ratios decreased in the order Pt/NaY (1.63) > Pt/MgY (1.55) > Pt/LaY (1.21) > Pt/H-USY (0.88). The average number of chemisorbed hydrogen atoms per surface Pt atoms (H/Pt_s) is obtained by dividing these values for the dispersion as calculated from the HRTEM experiments. The H/Pt_s values decreased in the same order (see Table 4).

4. Discussion

4.1. The geometrical structure of the Pt particles

EXAFS is a powerful and unique tool for providing the geometrical structure around the absorbing atom and obtaining information on particle size. The first-shell Pt–Pt coordination number of particles strongly depends on the size, because the number of atoms per particle increases with approximately the cube of particle diameter. However, when the particle size distribution is broad or bimodal, the larger particles dominate the average coordination number of the first-shell Pt–Pt. The deduced average particle size from EXAFS analysis in that case is an overestimation of the average diameter of the particle size distribution [26]. This means that using EXAFS to determine particle size is reliable only when the particle size distribution is narrow.

The results obtained from the HRTEM data indicate that for all samples, the Pt particle size distribution is relatively small, peaking around 1.1 nm. The Pt–Pt coordination number ($N_{Pt–Pt}$) can be calculated from the average Pt particle diameter as determined from the HRTEM data. Table 4 shows that the calculated values agree within the limits of accuracy with the Pt–Pt coordination numbers derived directly from the EXAFS data, with the largest deviation found for the Pt/NaY sample. This also implies that the assumptions for the calculations of spherical-shaped supported Pt particles with a face-centered cubic structure are correct.

Table 3 gives metal–oxygen distances ranging from 2.50 to 2.70 Å. Previous EXAFS studies on several supported metal catalysts (metals: Rh, Ir, Pt; supports: Al_2O_3, TiO_2, MgO, LTL, Y) [8,26,32] have demonstrated metal–oxygen interactions characterized by both short (2.10–2.20 Å) and long (2.5–2.8 Å) distances [31]. Combining the results of temperature-programmed desorption and EXAFS experiments, Vaarkamp et al. [32] concluded that the long metal–oxygen distance was due to the presence of hydrogen in the metal–support interface, because evacuation led to a shortening of this distance. Further proof of this was obtained from the EXAFS experiments carried out on Ir/Al_2O_3 catalysts [31]. The long metal–oxygen distance was shown to be reversible: admission of hydrogen after the evacuation treatment restored the originally observed long metal–oxygen distance. The long metal–oxygen distance observed in this work is therefore attributed to the metal–oxygen coordination arising from the metal–support interface. It should be

Table 4
Correlation between H/M experiments, dispersion (HRTEM) and EXAFS. Determination of number of chemisorbed hydrogen atoms per surface Pt (H/Pt_s)

Sample	Pt loading[a] (wt%)	H/M experiments		HRTEM	EXAFS	Calculation		
		V_{H_2} (cc/g_{cat})	H/Pt	d (nm)	$N_{Pt–Pt}$	$N_{Pt–Pt}$	Pt_s/Pt	H/Pt_s
Pt/NaY	1.0	0.941	1.63	1.14	6.1	6.8	0.83	1.96
Pt/MgY	1.05	0.935	1.55	0.92	6.3	5.7	0.89	1.74
Pt/LaY	0.91	0.695	1.21	1.23	7.1	7.2	0.80	1.51
Pt/H-USY	1.0	0.505	0.88	1.26	7.4	7.3	0.79	1.11

[a] Weightpercents per gram of dry zeolite, calculated by weighing the applied volume of precursor solution.

noted here that the long distance systematically decreases with decreasing ionicity of the support. More research is needed to further explain this observed effect.

4.2. Relationship between hydrogen chemisorption and dispersion: role of spillover hydrogen

The hydrogen chemisorption literature on supported metal catalysts has always assumed that higher dispersion always leads to higher H/M values. If the support is inert or if metal particles with different sizes and dispersed on the same support are compared, then this assumption is correct. But if metal particles are dispersed on supports with different properties (e.g., ionicity of the support oxygen atoms), then this assumption is no longer valid. This finding can be demonstrated by calculating the number of chemisorbed hydrogen atoms per surface Pt atom (H/Pt_s) of the four Pt catalysts studied in this work. The results of this exercise are given in Table 4. The Pt particle dispersions are calculated from the HRTEM data, and these values are used to derive the H/Pt_s as given in the last row of Table 4. It can be seen that the H/Pt_s values decrease in the order 1.96 (Pt/NaY) > 1.68 (Pt/MgY) > 1.49 (Pt/LaY) > 1.1 (Pt/H-USY). There is a clear decreasing trend with decreasing electron richness of the support oxygen atom. This implies that the hydrogen chemisorption capacity of the Pt particles is determined not only by their dispersion, but also by the ionicity of the support oxygen.

Another factor that can significantly influence the total amount of chemisorbed hydrogen is the presence of spillover hydrogen. The amount of spillover hydrogen can be very large on supports with high amounts of Brönsted acid sites and will decrease greatly with increasing reduction temperatures [33]. The parameters that control the amount of spillover hydrogen are not yet fully understood. Our samples were prepared by impregnation. Samples prepared by ion exchange generally exhibit greater spillover because a greater number of protons are introduced by the reduction of Pt^{2+} ion-exchanged in NaY. In any case, for the impregnated samples used in this study, the Pt/H-USY sample demonstrated the lowest total adsorbed hydrogen level, whereas the highest amount of spillover is expected for this sample. So although a certain amount of spillover will occur, the trends for chemisorption of hydrogen as a function of support ionicity as obtained in this work are still valid.

4.3. Influence of ionicity of the support on the hydrogen chemisorption capacity of Pt

Recent work by our group has revealed that the nature of support effect involves a change in the electronic properties of the metal cluster, induced by and correlated with the electron richness of the support oxygen atoms. The experimental results obtained from EXAFS, X-ray photoelectron spectroscopy (XPS), and Fourier transform infrared spectroscopy (FTIR) of chemisorbed CO can be explained by a shift of the complete Pt density of states to higher energy (lower binding energy) on ionic (basic) supports [7,8,19]. A proposed MO scheme to explain the observed changes in the EXAFS data in more detail [17] was based on the idea that the location of the $6s, p$ interstitial bonding orbitals moves from the surface of the Pt particle (Pt supported on electron-rich O atoms, for ionic or basic supports) to the Pt–support interface (Pt supported on electron-poor O atoms, for acidic supports with protons or supports with more covalent cations). This concept was confirmed by recent DFT calculations showing that the support-induced changes of the electronic structure within a supported Pt particle affects the chemisorption of such adsorbates as H_2, CH_x, and O_2 on the surface of Pt particle [22]. According to the DFT calculations, the Pt–H bond strength is larger on supports with electron-rich oxygen atoms (basic), which implies greater H coverage on ionic supports than on covalent supports (acidic, with electron-poor O atoms). The H/Pt_s data presented in Table 4 show that the number of hydrogen atoms chemisorbed per surface Pt is highest for Pt particles on the most ionic (basic) support (NaY) and lowest for Pt particles on the most covalent (acidic) support (H-USY). This implies that the H/M data presented in this paper are a direct experimental proof of recently published DFT calculations [22]. Moreover, they are completely in line with previously published Pt EXAFS, XANES, XPS, and CO FTIR [7,8,19,23] data and confirm our interatomic potential model that was put forward as a basis for metal–support interaction [17].

It should be noted that the affect of the ionicity of the support oxygen atoms will level off with increasing Pt particle size. No direct catalytic data on the support influence on large Pt particles are available, but based on our study of the insulator-to-metal transition as a function of the support ionicity [21] the metal–support interaction is expected to level off for particles >2.5 nm.

4.4. Implications for Pt-catalyzed reactions as hydrogenolysis and hydrogenation

The influence of the support on the H coverage of Pt particles has important consequences for Pt-catalyzed reactions, such as hydrogenolysis and hydrogenation. It has been reported that increasing alkalinity of the support results in decreased turnover frequency (TOF) of neo-pentane hydrogenolysis and increased negative order in hydrogen partial pressure (from roughly −1.5 to −2.5). Moreover, also a compensation relation is observed for the hydrogenolysis kinetic data of Pt on supports with different ionicities. Using information on the dominant hydrogen adsorption sites (atop or n-fold) obtained from the Pt L_3 XANES, the previously reported neo-pentane hydrogenolysis kinetic data can be fully explained by assuming a higher H coverage on Pt with increasing support alkalinity [9]. These assumptions are fully supported by the results obtained in this study.

Saturation of aromatics (tetralin [17] and benzene [34]) and hydrogenation of other oxygenated alkenes catalyzed by

Pt on oxidic supports [35] also show a strong influence of the support ionicity. The ionicity of the support again will control the hydrogen coverage of the supported Pt particles. We will explore the consequences of this control on the kinetics of Pt-catalyzed hydrogenation reactions in forthcoming papers.

5. Summary

Zeolite Y-supported Pt catalysts were prepared by dry impregnation. HRTEM indicated a similar Pt particle size distribution for all samples, with an average Pt particle size of 0.98–1.26 nm. The results are in good agreement with the first-shell Pt–Pt coordination numbers as determined from EXAFS analysis. However, hydrogen chemisorption experiments revealed that the determined H/Pt values have no relationship with the Pt dispersion calculated from the HRTEM results. Using these calculated dispersion values, the number of chemisorbed hydrogen atoms per surface platinum atom (H/Pt_s ratio) can be obtained: 1.96 (Pt/NaY) > 1.68 (Pt/MgY) > 1.49 (Pt/LaY) > 1.1 (Pt/H-USY). This shows a clearly decreasing trend with decreasing electron richness of the support oxygen atom. The hydrogen chemisorption capacity of Pt is directly influenced by the ionicity of the support oxygen. The H/M results presented in this paper are completely in line with previously published Pt AXAFS, XANES, XPS, and CO FTIR data [7,8,23] and provide an experimental proof of our recently published DFT calculations [22]. They confirm the interatomic potential model [17] that we have proposed as a basis for metal–support interaction.

H/M experiments can provide direct information about metal dispersion if the support is inert or if metal particles with different sizes and dispersed on the same support are compared. However, they cannot do so if metal particles are dispersed on supports with different properties (e.g., ionicity of the support oxygen atoms).

Acknowledgments

The authors thank the scientific staff at HASYLAB Beamline X1.1 for their continuing interest and stimulating support. This work was funded by the Material Engineering Division of Toyota Motor Europe. Fruitful discussions with Yasuo Ikeda and Muriel Lepage of this division and with researchers at the Toyota Central R&D Labs Japan are also acknowledged.

References

[1] R.A. Dalla Betta, M. Boudart, in: J.W. Hightower (Ed.), Proceedings of 5th International Congress on Catalysis, vol. 2, North Holland, 1973, p. 1329.
[2] S.T. Homeyer, Z. Karpinski, W.M.H. Sachtler, J. Catal. 123 (1990) 60–73.
[3] A. de Mallmann, D. Barthomeuf, J. Chim. Phys. 87 (1990) 535–538.
[4] Z. Karpinski, S.N. Gandhi, W.M.H. Sachtler, J. Catal. 141 (1993) 337–346.
[5] Z. Xu, F.S. Xiao, S.K. Purnell, O. Alexeev, S. Kawi, S.E. Deutsch, B.C. Gates, Nature 372 (1994) 346–348.
[6] P. Reyes, I. Concha, M.E. König, J.L.G. Fierro, Appl. Catal. A 103 (1993) 5–16.
[7] B.L. Mojet, J.T. Miller, D.E. Ramaker, D.C. Koningsberger, J. Catal. 186 (1999) 373–386.
[8] D.C. Koningsberger, J. de Graaf, B.L. Mojet, D.E. Ramaker, J.T. Miller, Appl. Catal. A 191 (2000) 205–220.
[9] D.C. Koningsberger, M.K. Oudenhuijzen, J.A. van Bokhoven, D.E. Ramaker, J. Catal. 125 (2003) 178–191.
[10] G.C. Bond, Catal. Today 17 (1993) 399.
[11] F.G. Gault, Adv. Catal. 30 (1981).
[12] K. Foger, J.R. Anderson, J. Catal. 54 (1978) 318–335.
[13] Z. Zhang, T.T. Wong, W.M.H. Sachtler, J. Catal. 128 (1991) 13–22.
[14] G. Larsen, G.L. Haller, Catal. Lett. 3 (1989) 103–110.
[15] A.M. Ferrari, G. Pacchioni, J. Phys. Chem. 100 (1996) 9032–9037.
[16] A.P.J. Jansen, R.A. van Santen, J. Chem. Phys. 94 (1990) 6764.
[17] D.E. Ramaker, J. de Graaf, J.A.R. van Veen, D.C. Koningsberger, J. Catal. 203 (2001) 7–17.
[18] N. López, J. Chem. Phys. 114 (2001) 2355–2361.
[19] A.M.J. van der Eerden, T. Visser, Y. Ikeda, M. Lepage, D.C. Koningsberger, B.M. Weckhuysen, J. Amer. Chem. Soc. 127 (2005) 1530–1540.
[20] J. Kua, W.A. Goddard III, J. Phys. Chem. B 102 (1998) 9481–9491.
[21] D.E. Ramaker, M.K. Oudenhuijzen, D.C. Koningsberger, J. Phys. Chem. B 109 (2005) 5605–5617.
[22] M.K. Oudenhuijzen, J.A. van Bokhoven, D.E. Ramaker, D.C. Koningsberger, J. Phys. Chem. B 108 (2004) 20247–20254.
[23] M.K. Oudenhuijzen, J.A. van Bokhoven, J.T. Miller, D.E. Ramaker, D.C. Koningsberger, J. Amer. Chem. Soc. 127 (2005) 1530–1540.
[24] O.L.J. Gijzeman, A.J.M. Mens, J.J. van Lenthe, W. Mortier, B.M. Weckhuysen, J. Phys. Chem. B 107 (2003) 678.
[25] J.A. van Bohhoven, A.L. Roest, D.C. Koningsberger, J.T. Miller, G.H. Nachtegaal, A. Kentgens, J. Phys. Chem. B 104 (2000) 6743–6754.
[26] J. De Graaf, A.J. van Dillen, K.P. de Jong, D.C. Koningsberger, J. Catal. 203 (2001) 307–321.
[27] M. Vaarkamp, B.L. Mojet, M.J. Kappers, J.T. Miller, D.C. Koningsberger, J. Phys. Chem. B 99 (1995) 633–636.
[28] M. Vaarkamp, J.C. Linders, D.C. Koningsberger, Physica B 208/209 (1995) 159–160.
[29] D.C. Koningsberger, B.L. Mojet, G.E. van Dorssen, D.E. Ramaker, Top. Catal. 10 (2000) 143–155.
[30] E.H. Voogt, Nubie Computer Program, Debye Institute of Utrecht University, 1996.
[31] D.C. Koningsberger, F.B.M. van Zon, M. Vaarkamp, A. Muñoz-Paez, in: Y. Iwasawa (Ed.), X-Ray Absorption Fine Structure for Catalysts and Surfaces, Tokyo, 1995, P257.
[32] M. Vaarkamp, F.S. Modica, J.T. Miller, D.C. Koningsberger, J. Catal. 144 (1993) 611.
[33] J.T. Miller, B.L. Meyers, F.S. Modica, G.S. Lane, M. Vaarkamp, D.C. Koningsberger, J. Catal. 143 (1993) 395.
[34] S.D. Lin, M.A. Vannice, J. Catal. 143 (1993) 563.
[35] M.A. Vannice, D. Poondi, J. Catal. 169 (1997) 166.